Deep Learning-based Group Causal Inference in Multivariate Time-series

Wasim Ahmad, Maha Shadaydeh, Joachim Denzler

Computer Vision Group, Faculty of Mathematics and Computer Science,
Friedrich Schiller University Jena, Germany
{wasim.ahmad, maha.shadaydeh, joachim.denzler}@uni-jena.de

Abstract

Causal inference in a nonlinear system of multivariate time series is instrumental in disentangling the intricate web of relationships among variables, enabling us to make more accurate predictions and gain deeper insights into real-world complex systems. Causality methods typically identify the causal structure of a multivariate system by considering the cause-effect relationship of each pair of variables while ignoring the collective effect of a group of variables or interactions involving more than two-time series variables. In this work, we test model invariance by group-level interventions on the trained deep networks to infer causal direction in groups of variables, such as climate and ecosystem, brain networks, etc. Extensive testing with synthetic and real-world time series data shows a significant improvement of our method over other applied group causality methods and provides us insights into real-world time series. The code for our method can be found at: https://github.com/wasimahmadpk/gCause.

Introduction

Group-based causal inference investigates causal relationships within specific groups of individuals, entities, or units. It is particularly relevant when studying complex systems with interconnected components such as in climate (Molotoks et al. 2020) and brain networks (Faes et al. 2022), allowing researchers to investigate how variables within distinct groups contribute to observed outcomes or behaviors. In this paper, we explore the fundamental concept behind group-based causal inference in multivariate time series and its growing significance in diverse disciplines. To this end, we present our approach to testing the causal link in groups of time series, see Figure 1, which provides a comprehensive understanding of how these groups interact. The proposed method allows the testing of bi-directional causal links. Our method builds on our previous work (Ahmad, Shadaydeh, and Denzler 2022), which exploits the model invariance property through Knockoffs (Barber and Candès 2015, 2019; Barber, Candès, and Samworth 2020) interventions for pairs of variables in deep networks for causal estimation. However, here we emphasises the identification of causal interaction in groups of variables and is the first group
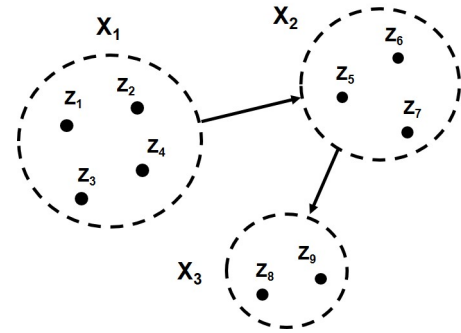
Figure 1: Interactions among groups of multivariate time series data of various dimensions.

causality method to the best of our knowledge which utilize deep learning to learn complex nonlinear relation. The model invariance property refers to the invariant behavior of the model in different settings when its causal predictors are observed (Peters, Bühlmann, and Meinshausen 2016). We use DeepAR (Salinas et al. 2020) to model multivariate time series which has the potential to learn complex interactions in nonlinear data. Since deep networks cannot handle missing variables or adjust to out-of-distribution data, we use Knockoff variables for interventions on the trained deep networks. Knockoffs are in-distribution, uncorrelated copies of the original data with similar covariance structure.

To demonstrate the robustness and practical utility of our approach, we evaluate its performance on synthetically generated time series and real-world datasets. We compare our method with other group causality methods, i.e., Vanilla-PC (Janzing, Hoyer, and Schölkopf 2009), Trace method (Zscheischler, Janzing, and Zhang 2012) and 2GVecCI (Wahl, Ninad, and Runge 2023). As a real-world application, we mainly focus on the climate system and assessing the direction of connections in brain networks. This involves considering the internal processes over a period of time involving interactions within and between different climate subsystems, i.e., ocean, land, ecosystem, atmosphere, etc. (Latif and Keenlyside 2009). For example, how climate and ecosystem interact (Malhi et al. 2020; Sefidmazgi and Sefidmazgi 2020; Korell et al. 2020), or how major climate phenomena such as the El Niño Southern Oscilla-

tion (ENSO) affect different global regions (Nowack et al. 2020). These highly complex interactions provide the basis for understanding the profound impacts of environmental change. We conducted experiments on the FLUXNET data (Pastorello et al. 2020), which contains measurements from different sites that capture climate-ecosystem dynamics, where we aim to uncover the causal pathways between climate and ecosystem. We have also tested our method on a climate science dataset (ENSO 3.4), where we aim to estimate the impact of temperature patterns in the tropical Pacific on British Columbia. Moreover, we apply our method to simulated fMRI time series to identify connections in the brain network and indicate their directionality.

Related Work

There are many methods for time series causal inference with applications in various fields that rely on certain assumptions that limit their applicability (Yao et al. 2020). These approaches treat each system variable separately and estimate its causal relation to other variables, overlooking the group or collective influence, e.g., causal relation in brain regions (Siddiqi et al. 2022), ecosystem and climate subsystems, etc. The work of (Besserve et al. 2018) presents a group theoretical framework to assess the relationship between cause and mechanism using group transformations. Vanilla-PC (Janzing, Hoyer, and Schölkopf 2009) estimates the direction of a causal link in two groups of time series; however, the method suffers from high dimensionality in terms of accuracy and computation time because it runs a higher number of conditional independence tests. The Trace method is introduced by (Zscheischler, Janzing, and Zhang 2012) to infer causal direction in two linearly interacting groups which works faster, however, its performance degrades in case of high nonlinear relationships in groups. The authors of (Wahl, Ninad, and Runge 2023) present 2GVecCI for uni-directional causality between two groups where they combine the constraint-based approach for causal discovery with sparsity measures of the internal causal structure of the groups. The 2GVecCI method is based on two principles for causal relations between groups of time series. First, conditioning on the cause group does not lead to new conditional dependencies within the effect group. Second, conditioning on the effect group does not delete conditional dependencies within the cause group.

The authors of (Faes et al. 2022) assess higher-order interactions in networks of processes through time and frequency domain analysis. The work of (Sato et al. 2010) uses Granger causality for a set of time series to analyze the connectivity between brain regions, assuming that sets are linearly related to each other while real-world data are highly nonlinear. Approaches that depend on the non-Gaussian nature of noise for drawing conclusions about causal direction, for example, LinGaM (Shimizu et al. 2006), become less effective due to the influence of averaging caused by the central limit theorem, which tends to make the averaged noise distribution more Gaussian. Furthermore, methods for group causality aim to transform data by aggregation or dimensionality reduction, where a significant amount of information may be lost and, more importantly, the exist-

ing causal structure (Spirtes, Glymour, and Scheines 2000) is disrupted. However, our work utilizing deep networks has the potential to learn complex relationships in high-dimensional data. For brain data, the detection of networks and their directions using fMRI time series is of high interest. The work of (Smith et al. 2011) presents various correlation and causality-based method to identify the association between brain network nodes and assign a direction to them. They generate realistic simulated fMRI data for a wide range of underlying networks and experimental protocols to compare different connectivity estimation approaches.

Method

In this section, we present the formulation of our method for group causal discovery assessing the causal relationships within sets of N-variate system of time series denoted as $Z^N = \{Z_1, \ldots, Z_N\}$. These variables are organized into G groups or subsets of variables, represented as $X^G = \{X_1, \ldots, X_G\}$, which can be considered as indicative of the behavior of a network comprising G distinct dynamic subsystems. Referring to the real-world applications, the groups $X_i, i = 1, \ldots, G$ may represent subsets of the climate system, brain networks, etc., where each group process $Z_{t,t=1,\ldots,n}$, may represent the intra-atmospheric interaction or neural activity of a brain region. Each of these groups $X_i : Z \subset Z^N$ has a certain dimension G_i, such that the total number of variables N can be expressed as $N = \sum_{i=1}^{G} G_i$. The method allows the assessment of uni- and bi-directional causal links in any number of groups. For two causally related groups $X_i, X_j, i, j = 1, \ldots, G$ where $i \neq j$, the possible links can be $X_i \xrightarrow{\text{causes}} X_j$, or $X_j \xrightarrow{\text{causes}} X_i$ or $X_i \xleftrightarrow{\text{causes}} X_j$.

Assumptions We infer causal relationships in groups of nonlinear multivariate time series by making the following assumptions:

- Stationarity: The variables Z^N represent a stochastic stationary process.
- Causal Sufficiency: The set of observed variables $Z^N = \{Z_1, \ldots, Z_N\}$ contain all common causes in Z^N, i.e., no hidden confounders.
- Model Invariance: The causal structure in the stochastic processes Z^N remains consistent across different interventional enviroments.

The presented method for group causality in time series builds on our previous work (Ahmad, Shadaydeh, and Denzler 2022) where we model the complex interactions in N-variate time series by training deep networks and apply model invariance testing through group-level interventions for inferring causal direction in groups. A model is invariant if, in the presence of its causal predictors, the distribution of its output residuals does not change across interventional environments (Peters, Bühlmann, and Meinshausen 2016). The schematic diagram for our method is shown in Figure 2, where we apply invariance testing to deep networks trained on sets of time series in order to infer causality in groups. Through deep autoregressive models (Salinas et al. 2020) which takes $Z^N =$
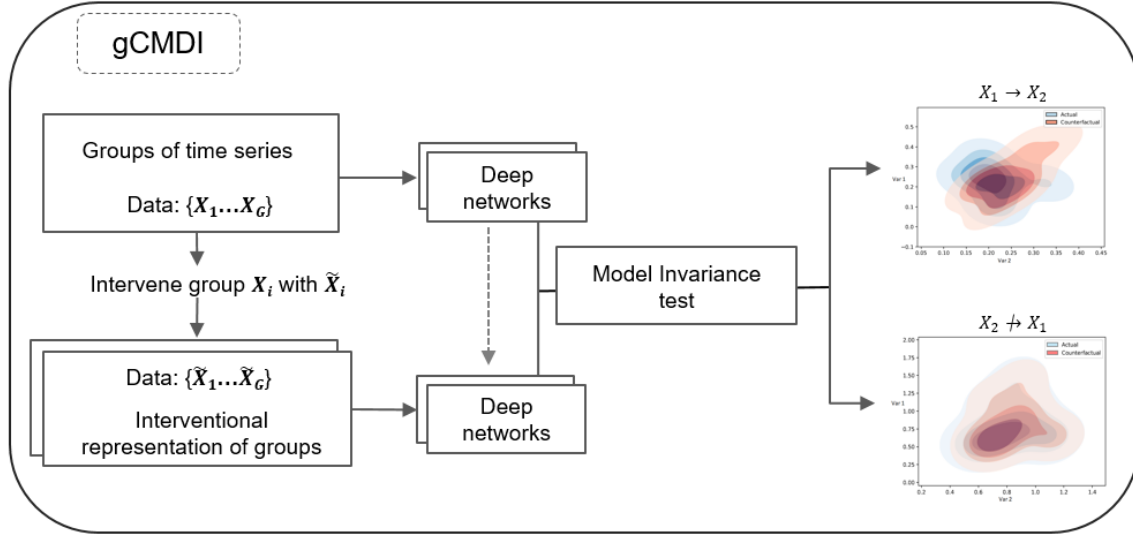
Figure 2: Schematic diagram of group causal discovery method where we model the complex relation among all variables in the system with deep learning approximator. For group-level causal inference, we implement model invariance testing by applying intervention to a group of interest and estimate its influence on the target group.
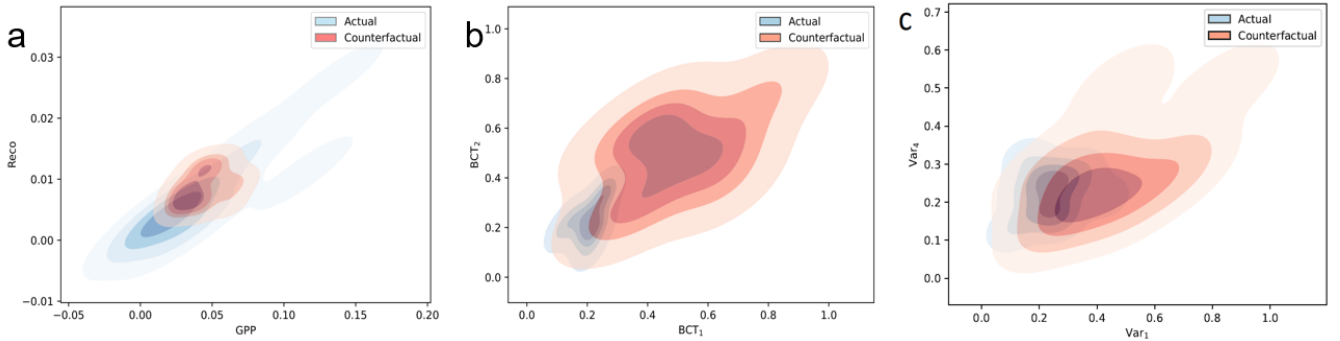

Figure 3: Distribution shift of **a**. ecosystem group $G_{\mathrm{E}} = \{GPP, R_{\mathrm{eco}}\}$ in response to intervention on climate group $G_{\mathrm{C}} = \{T, R_g\}$. **b**. British Columbia temperature in response to intervention on ENSO temperature data. **c**. Brain network N_2 in fMRI time series after group-level intervention on network N_1.

$\{Z_1, \ldots, Z_N\}$ as input, we model the conditional distribution $P(Z_{i,t_0:T}|Z_{i,1:t_0-1}, Z_{-i,1:t_0-1}), i = 1, \ldots, N$ of the future of all system variables given their past values. Here Z_i represents node of the target group and Z_{-i} refers to the nodes in the rest of the groups in X^G. It utilizes recurrent neural networks (RNNs) to generate probabilistic output in terms of μ and σ^2 at each time point where the mean represents the central estimate, and the variance represents the uncertainty of the system. For all variables, we obtain distribution R of their residuals $e^n = e_1, \ldots, e_n$ for n forecast windows where $e = \frac{1}{T}\sum_{t=1}^{T}|\frac{Z_t - Z_{pred}}{Z_t}|$ and T represents forecast horizon. Pertaining to the invariance property, the model response Z_i, which is the target group of variables, does not change in different settings as long as we don't perturb the cause group.

Knockoff Intervention The effectiveness of our previously proposed Knockoff intervention (Barber and Candès 2015, 2019; Barber, Candès, and Samworth 2020) compared to other intervention methods is demonstrated on node-to-node causal relationship in multivariate time series (Ahmad, Shadaydeh, and Denzler 2021, 2022). Let's say X_j represent the group of output variables of the trained deep network, and X_i denotes the input group where $i \neq j$. The causal effect of group X_i on the network output group X_j under intervention is denoted as:

$$E(X_j|do(X_i = \tilde{X}_i)) \qquad (1)$$

where $\tilde{X}_i$ is a knockoff representation or configuration to which the group of variables X_i is set. Note that group X_i contains internal process or nodes $Z_t, t = 1, \ldots, n$. Each node within a group is replaced with the generated knockoff copies. Applying the do-operator on trained deep
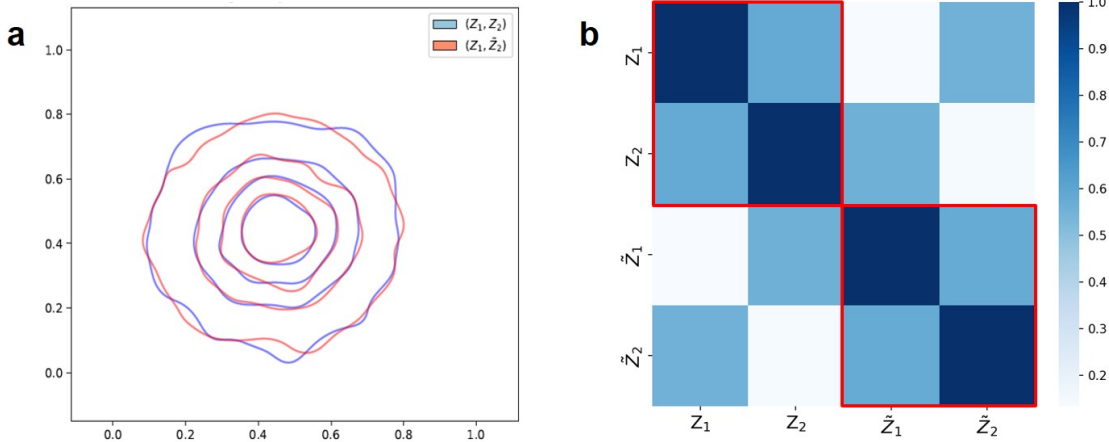
Figure 4: **a**. Illustration of exchangeability property $(Z_1, Z_2) \overset{d}{=} (Z_1, \tilde{Z}_2)$ of knockoff variables **b**. Shows the correlation matrix $\Sigma_{Z\tilde{Z}}$ of the original variables Z and knockoffs $\tilde{Z}$ where the sub-matrix for the correlation within the generated knockoffs $\Sigma_{\tilde{Z}_1\tilde{Z}_2}$ is similar to that of correlation in original variables $\Sigma_{Z_1 Z_2}$, enclosed in red squares. While the variable-wise correlation is minimized with their respective knockoff copies, i.e., $\sigma_{Z_1\tilde{Z}_1}, \sigma_{Z_2\tilde{Z}_2} \approx 0$, shown in white squares.

networks involves specifying interventions or changes to the input group of time series to observe the corresponding effects on the target group. This implies that, instead of observing the natural variation in X_i, we are setting it to knockoff version $\tilde{X}_i$ in order to assess the collective causal impact on the network's output. We choose to use multivariate Gaussian model within the Knockoff framework which implements semidefinite programming (SDP) to estimate knockoff parameters given the mean μ_Z and covariance matrix Σ_Z of the original variables Z. We generate knockoff copies $\tilde{Z}_1, \ldots, \tilde{Z}_N$ as an interventional representation of $Z_1, \ldots, Z_N$, which are used to replace variables during an intervention. The generated knockoff variables are in-distribution and uncorrelated with the original variables. Moreover, it fulfills the exchangeability condition $(Z_i, \tilde{Z}_j) \overset{d}{=} (\tilde{Z}_i, Z_j), i, j = 1, \ldots, N, i \neq j$ (Barber and Candès 2019) by maintaining same covariance structure as the original time series, which means that the underlying joint distribution of the data does not change by replacing a variable with its knockoff copy. The properties of knockoffs are demonstrated in Figure 4.

Group Causal Inference In order to infer causal direction in two groups of variables, i.e., $X_i \rightarrow X_j$, we apply Kolmogorov–Smirnov (KS) test (Smirnov 1939)

$$C_{ij} = \sqrt{\frac{qr}{q+r}} sup|R - \widetilde{R}| \qquad (2)$$

to evaluate model invariance property by estimating the maximum absolute difference in the marginal residual distribution R and $\widetilde{R}$ of variables in X_j before and after group-level intervention on X_i. Here $\widetilde{R}$ represents the distribution of the residuals $\widetilde{e}^n = \widetilde{e}_1, \ldots, \widetilde{e}_n$, obtained while esti-

mating the counterfactuals $P(Z_{i,t_0:T}|Z_{i,1:t_0-1}, \widetilde{Z}_{-i,1:t_0-1})$. The KS test uses a significance level α and other parameters like q, r which represents the number of samples in marginal residual distributions R and $\widetilde{R}$. The test statistic C is used to calculate p value for deciding whether a causal link exists or not. If $p_{ij} > \alpha$, the null hypothesis H_0: X_i does not cause X_j is accepted, which means that the residual distributions of group of variables before and after intervention are approximately identical across various interventional settings, i.e., the group invariance property is fulfilled. In the alternate case, the null hypothesis is rejected, i.e. H_1: X_i causes X_j. We test for both causal links $X_i \rightarrow X_j$ and $X_j \rightarrow X_i$ for all possible values of i, j where $i \neq j$. It is important to mention that if a single node within the group is influenced by its causal group, it establishes a causal connection between the groups and it doesn't necessarily imply that the entire target group is uniformly affected by its cause.

Experiments

Synthetic Data To evaluate the performance of our method, we use synthetic data model $Z_t^j = \Sigma_i f_i(Z_{t-k}^i) + \eta_t^j$, $i, j = 1, ..., N, 0 < k < t$. The system variables Z_j have auto and cross-functional dependencies with a time delay of k. The data model incorporates linear and nonlinear dependencies f, i.e., exponential, polynomial with varying edge densities, and adds uncorrelated, normally distributed noise η_t^j. We incorporate inter- and intra-group causal links in the generated causal graphs. The decision of the methods for each edge in the groups is either *correct*, *wrong* or *no inference*. Our method (gCDMI) achieves better identification of the correct causal links with fewer wrong detections in subsystems for all edge densities, i.e., sparse to dense causal graphs, as compared to other group causality meth-

Table 1: Performance of the applied methods on synthetic data for varying interaction densities. The presented values are the ratio of the method output and the total number of tests where the *Correct* inference represents the true causal direction, *Wrong* is the opposite of the true causal direction, and *No inference* is reporting the absence of a causal link.

Method	Inference	Interaction density								
		0.2	0.3	0.4	0.5	0.6	0.7	0.8	0.9	1.0
gCDMI	Correct	**1.00**	0.67	**1.00**	**1.00**	**1.00**	**0.67**	0.67	**1.00**	**1.00**
	Wrong	**0.00**	0.33	**0.00**	**0.00**	**0.00**	0.33	0.33	**0.00**	**0.00**
	No inference	**0.00**	**0.00**	**0.00**	**0.00**	**0.00**	**0.00**	**0.00**	**0.00**	**0.00**
Trace	Correct	0.67	**1.00**	0.67	0.67	0.67	**0.67**	0.67	**1.00**	0.67
	Wrong	0.33	**0.00**	0.33	0.33	0.33	0.33	0.33	**0.00**	0.33
	No inference	**0.00**	**0.00**	**0.00**	**0.00**	**0.00**	**0.00**	**0.00**	**0.00**	**0.00**
2GVecCI	Correct	0.67	0.00	**1.00**	0.33	0.67	0.33	**1.00**	0.67	0.00
	Wrong	0.33	0.33	**0.00**	0.33	**0.00**	**0.00**	**0.00**	**0.00**	0.33
	No inference	**0.00**	0.67	**0.00**	0.33	0.33	0.67	**0.00**	0.33	0.67
Vanilla-PC	Correct	0.67	0.67	0.67	0.33	0.67	**0.67**	0.33	0.33	0.00
	Wrong	**0.00**	**0.00**	0.33	0.33	**0.00**	0.33	0.67	0.67	1.00
	No inference	0.33	0.33	**0.00**	0.33	0.33	**0.00**	**0.00**	**0.00**	**0.00**

Table 2: Performance of different group causality methods in identifying causal direction in climate-ecosystem data for various sites. Here ✓ indicates the presence of the link, while × indicates the absence of the link and → represents the direction of causal relation between groups. We test a bi-directional causal link only for our method.

Sites	Inference	Methods			
		gCDMI	Trace	V-PC	2GVCI
DE-Hai	$G_C \rightarrow G_E$	×	×	×	×
	$G_C \leftarrow G_E$	×	✓	×	×
	$G_C \leftrightarrow G_E$	✓	–	–	–
	$G_C \nleftrightarrow G_E$	×	×	✓	✓
IT-MBo	$G_C \rightarrow G_E$	✓	✓	✓	×
	$G_C \leftarrow G_E$	×	×	×	×
	$G_C \leftrightarrow G_E$	×	–	–	–
	$G_C \nleftrightarrow G_E$	×	×	×	✓
FR-Pue	$G_C \rightarrow G_E$	✓	×	×	×
	$G_C \leftarrow G_E$	×	✓	×	×
	$G_C \leftrightarrow G_E$	×	–	–	–
	$G_C \nleftrightarrow G_E$	×	×	✓	✓
US-Ton	$G_C \rightarrow G_E$	✓	×	×	×
	$G_C \leftarrow G_E$	×	✓	×	✓
	$G_C \leftrightarrow G_E$	×	–	–	–
	$G_C \nleftrightarrow G_E$	×	×	✓	×

ods as shown in Table 1. The given values are the ratio of the method decision and the total number of experiments. It can be noticed that our method reported only fewer wrong inferences and zero *no inference* along with the Trace method for all experiments, while other methods reported *no inference* in a number of tests because they are uni-directional and sometimes it is hard to distinguish cause from effect when the interaction in both directions is not significantly different. We also found that increasing edge density does not have a clear impact on the outcome except for Vanilla-PC, where the performance is degraded. We used multiple group dimensions for each edge density in our experiments,

where we vary the architecture of the deep networks based on group dimension. All experiments in this paper were conducted on an NVIDIA GeForce RTX 3060 Ti graphics card, providing reliable performance capabilities for complex synthetic and real-world data causal analysis. The improved performance of our method comes at the cost of high computation time due to its dependence on deep networks to learn complex causal structures in data.

FLUXNET Data Here, we aim to perform a causal analysis of environmental time series with our method by establishing the causal structure in groups or subsystems. We carry out experiments with FLUXNET2015 dataset (Pastorello et al. 2020), which is acquired using the eddy covariance technique to measure the cycling of carbon, water, and energy between the biosphere and atmosphere through collaborations among many regional networks, with data preparation efforts happening at site and network levels. For our experiments, we considered various measurement sites, i.e., Hainich (DE-Hai: Deciduous Broadleaf Forests), Monte Bondone (IT-MBo: Grasslands), Puechabon (FR-Pue: Evergreen Broadleaf Forests), and Tonzi Ranch (US-Ton: Woody Savannas) site. The dataset includes climatic and ecological time series, i.e., global radiation (R_g), temperature (T), gross primary production (GPP), ecosystem respiration (R_{eco}) for various time scales i.e., half-hourly, hourly, daily, weekly and so on. We categorized these variables into two groups: climate group G_C which contains T and R_g and ecosystem group G_E, which consists of the ecosystem variables GPP and R_{eco}. We considered daily sampling which is advantageous for mitigating the effects of daily patterns that usually undermine the underlying causal relation in data. The results for all applied causality methods from various sites are given in Table 2. Our method identified the presence of a causal link $G_C \rightarrow G_E$ for all sites except for the DE-Hai site where we obtain a bidirectional link $G_C \leftrightarrow G_E$ which is an overall better performance compared to other methods. The bidirectional link at the DE-Hai

site, which is a deciduous broadleaf forest, could be due to climate-ecosystem strong feedback mechanism or other influential factors that need further investigation. For DE-Hai, Vanilla-PC and 2GVecCI could not infer any causal direction while the Trace method detected $G_E \rightarrow G_C$. For IT-MBo, all methods correctly identified the expected causal directions except 2GVecCI. As an illustration, we show climatic influence on the ecosystem for the IT-MBo site from one of our experiments in Figure 3 (a).

ENSO Data Moreover, we performed experiments on the ENSO dataset where we consider surface temperatures over the ENSO region and British Columbia (BCT) from 1948 to 2021, as a causal effect of temperatures in the tropical Pacific on those in North America is recognized in climate (Taylor 1998). During an El Niño event, which is one phase of ENSO, the tropical Pacific Ocean warms up significantly, disrupt normal weather patterns and influence the climate in other parts of the world, including the British Columbia region. For experiments, we adapted data preprocessing, i.e., deseasonalizing, smoothing, and aggregation from the work of (Runge et al. 2019; Wahl, Ninad, and Runge 2023). We show results for applied group causality methods in Table 3. Both our method and 2GVecCI identified significant influence of ENSO on BCT for various grid scales with a fraction of 0.66 correct inferences and 0.34 as no inferences. While Trace method detected the causal link ENSO $\rightarrow$ BCT with a fraction of 0.50 correct inferences and 0.50 wrong inferences. Vanilla-PC could not inferred any causal direction for all grid scales that is probably because of difficultly in distinguishing data patterns at both regions. Illustration of the causal influence of ENSO on BCT for one of the performed tests by our method is given in Figure 3 (b). Which shows the comparison of the BCT distribution with and without group-level intervention on the ENSO time series variables. The shift in the counterfactual distribution for BCT is indicative of the influence of ENSO.

Table 3: Effect of surface temperature at Tropical Pacific ocean (ENSO region) on British Columbia region, computed at various grid scales. The given values represent the decision of the applied methods (in percentage).

Inference	gCDMI	Trace	2GVCI	V-PC
ENSO $\rightarrow$ BCT	**0.66**	0.50	**0.66**	0.00
ENSO $\leftarrow$ BCT	**0.00**	0.50	**0.00**	**0.00**
ENSO $\leftrightarrow$ BCT	0.34	**0.00**	0.34	1.00

fMRI Data We analyzed simulated fMRI time series data (Smith et al. 2011) to identify connections in brain network nodes and assign direction to them. These fMRI time series simulations were based on dynamic causal modelling (DCM) (Friston, Harrison, and Penny 2003) fMRI forward model. The generated dataset provides ground truth connectivity graph for variety of network topologies which we use to evaluate our methods. Here we conducted experiments on a number of simulated subjects from $S2$ topology in the dataset which contains 10 nodes clustered into 2 groups. It has 10 min fMRI sessions for each subject with 3 sec sam-

pling rate, final added noise of 1%, and haemodynamic response function (HRF) variability of ±0.5 which provides time series of 200 data points. The percentage of methods outcome in terms of *correct*, *wrong* and *no inference* is given in Table 4. Since our method is data demanding as it relies on deep networks, the provided size of time series was not long enough for our method to learn the complex relationship properly. Determining the correct directionality of connections in fMRI time series is challenging because of the complex interactions among brain networks. However, our approach inferred correct direction 56% of the times in brain networks with 21% bidirectional links which is overall better performance compared to other applied group causality methods. Results from Trace method were somehow comparable to that of gCDMI. While 2GVecCI and Vanilla-PC yielded high percentage of *no inference* probably because of difficulty in separating cause from effect in a mutual interaction scenario between groups. The causal influence of brain network N_1 on network N_2 for one subject in $S2$ topology from simulated fMRI time series is demonstrated in Figure 3 (c).

Table 4: Identification of the direction of brain network connections using simulated fMRI time series by the applied group causality methods: Ground truth network connection: $N_1 \rightarrow N_2$. The given values represent the decision of the applied methods (in percentage).

Inference	gCDMI	Trace	2GVCI	Vanilla-PC
$N_1 \rightarrow N_2$	**0.56**	0.50	0.33	0.06
$N_1 \leftarrow N_2$	0.17	0.39	0.17	**0.16**
$N_1 \leftrightarrow N_2$	**0.21**	-	-	-
$N_1 \nleftrightarrow N_2$	**0.06**	0.11	0.50	0.78

Conclusion

In this work, we have introduced a deep learning-based method to uncover the causal interactions in groups or subsets of time series. We model complex relationships in an N-variable system of time series using deep learning models, and apply invariance testing via group-level intervention to infer causal direction in groups of variables. Our approach also tests for bi-directional causal links which signify a mutual influence, suggesting that the variables have a reciprocal cause-and-effect relationship. While our approach demonstrated improved performance on both synthetic and real-word time series data compared to other causality methods, it is worth noting that the high computational time is a trade-off inherent to its reliance on deep learning. As future work, we consider estimating the causal interactions in more than two groups of time series. Moreover, we aim to address the issue of non-stationarity and hidden confounding (Trifunov, Shadaydeh, and Denzler 2022) to further improve our method.

Acknowledgments

dation within the scope of the program line "Breakthroughs: Exploring Intelligent Systems" for "Digitization — explore the basics (No P2017-01-003), use applications".

References

Ahmad, W.; Shadaydeh, M.; and Denzler, J. 2021. Causal Inference in Non-linear Time-series using Deep Networks and Knockoff Counterfactuals. In *2021 20th IEEE International Conference on Machine Learning and Applications (ICMLA)*, 449–454. IEEE.

Ahmad, W.; Shadaydeh, M.; and Denzler, J. 2022. Causal Discovery using Model Invariance through Knockoff Interventions. In *ICML 2022: Workshop on Spurious Correlations, Invariance and Stability*.

Barber, R. F.; and Candès, E. J. 2015. Controlling the false discovery rate via knockoffs. *The Annals of Statistics*, 43(5): 2055–2085.

Barber, R. F.; and Candès, E. J. 2019. A knockoff filter for high-dimensional selective inference. *The Annals of Statistics*, 47(5): 2504–2537.

Barber, R. F.; Candès, E. J.; and Samworth, R. J. 2020. Robust inference with knockoffs. *The Annals of Statistics*, 48(3): 1409–1431.

Besserve, M.; Shajarisales, N.; Schölkopf, B.; and Janzing, D. 2018. Group invariance principles for causal generative models. In *International Conference on Artificial Intelligence and Statistics*, 557–565. PMLR.

Faes, L.; Mijatovic, G.; Antonacci, Y.; Pernice, R.; Barà, C.; Sparacino, L.; Sammartino, M.; Porta, A.; Marinazzo, D.; and Stramaglia, S. 2022. A new framework for the time-and frequency-domain assessment of high-order interactions in networks of random processes. *IEEE Transactions on Signal Processing*, 70: 5766–5777.

Friston, K. J.; Harrison, L.; and Penny, W. 2003. Dynamic causal modelling. *Neuroimage*, 19(4): 1273–1302.

Janzing, D.; Hoyer, P. O.; and Schölkopf, B. 2009. Telling cause from effect based on high-dimensional observations. *arXiv preprint arXiv:0909.4386*.

Korell, L.; Auge, H.; Chase, J. M.; Harpole, S.; and Knight, T. M. 2020. We need more realistic climate change experiments for understanding ecosystems of the future. *Global Change Biology*, 26(2): 325–327.

Latif, M.; and Keenlyside, N. S. 2009. El Niño/Southern Oscillation response to global warming. *Proceedings of the National Academy of Sciences*, 106(49): 20578–20583.

Malhi, Y.; Franklin, J.; Seddon, N.; Solan, M.; Turner, M. G.; Field, C. B.; and Knowlton, N. 2020. Climate change and ecosystems: Threats, opportunities and solutions.

Molotoks, A.; Henry, R.; Stehfest, E.; Doelman, J.; Havlik, P.; Krisztin, T.; Alexander, P.; Dawson, T. P.; and Smith, P. 2020. Comparing the impact of future cropland expansion on global biodiversity and carbon storage across models and scenarios. *Philosophical Transactions of the Royal Society B*, 375(1794): 20190189.

Nowack, P.; Runge, J.; Eyring, V.; and Haigh, J. D. 2020. Causal networks for climate model evaluation and constrained projections. *Nature communications*, 11(1): 1415.

Pastorello, G.; Trotta, C.; Canfora, E.; Chu, H.; Christianson, D.; Cheah, Y.-W.; Poindexter, C.; Chen, J.; Elbashandy, A.; Humphrey, M.; et al. 2020. The FLUXNET2015 dataset and the ONEFlux processing pipeline for eddy covariance data. *Scientific data*, 7(1): 1–27.

Peters, J.; Bühlmann, P.; and Meinshausen, N. 2016. Causal inference by using invariant prediction: identification and confidence intervals. *Journal of the Royal Statistical Society: Series B (Statistical Methodology)*, 78(5): 947–1012.

Runge, J.; Nowack, P.; Kretschmer, M.; Flaxman, S.; and Sejdinovic, D. 2019. Detecting and quantifying causal associations in large nonlinear time series datasets. *Science Advances*, 5(11): eaau4996.

Salinas, D.; Flunkert, V.; Gasthaus, J.; and Januschowski, T. 2020. DeepAR: Probabilistic forecasting with autoregressive recurrent networks. *International Journal of Forecasting*, 36(3): 1181–1191.

Sato, J. R.; Fujita, A.; Cardoso, E. F.; Thomaz, C. E.; Brammer, M. J.; and Amaro Jr, E. 2010. Analyzing the connectivity between regions of interest: an approach based on cluster Granger causality for fMRI data analysis. *Neuroimage*, 52(4): 1444–1455.

Sefidmazgi, M. G.; and Sefidmazgi, A. G. 2020. Causality Analysis of Climate and Ecosystem Time Series. In *Evaluating Climate Change Impacts*, 139–162. Chapman and Hall/CRC.

Shimizu, S.; Hoyer, P. O.; Hyvärinen, A.; Kerminen, A.; and Jordan, M. 2006. A linear non-Gaussian acyclic model for causal discovery. *Journal of Machine Learning Research*, 7(10).

Siddiqi, S. H.; Kording, K. P.; Parvizi, J.; and Fox, M. D. 2022. Causal mapping of human brain function. *Nature reviews neuroscience*, 23(6): 361–375.

Smirnov, N. V. 1939. On the estimation of the discrepancy between empirical curves of distribution for two independent samples. *Bull. Math. Univ. Moscou*, 2(2): 3–14.

Smith, S. M.; Miller, K. L.; Salimi-Khorshidi, G.; Webster, M.; Beckmann, C. F.; Nichols, T. E.; Ramsey, J. D.; and Woolrich, M. W. 2011. Network modelling methods for FMRI. *Neuroimage*, 54(2): 875–891.

Spirtes, P.; Glymour, C. N.; and Scheines, R. 2000. *Causation, prediction, and search*. MIT press.

Taylor, W. G. 1998. *Effect of El Nino Southern Oscillation (ENSO) on British Columbia and Yukon winter weather*. Aquatic and Atmospheric Science Division, Pacific and Yukon Region . . . .

Trifunov, V.-T.; Shadaydeh, M.; and Denzler, J. 2022. Time Series Causal Link Estimation under Hidden Confounding using Knockoff Interventions. In *A causal view on dynamical systems, NeurIPS 2022 workshop*.

Wahl, J.; Ninad, U.; and Runge, J. 2023. Vector causal inference between two groups of variables. In *Proceedings of the AAAI Conference on Artificial Intelligence*, volume 37, 12305–12312.

Yao, L.; Chu, Z.; Li, S.; Li, Y.; Gao, J.; and Zhang, A. 2020. A Survey on Causal Inference. arXiv:2002.02770.

Zscheischler, J.; Janzing, D.; and Zhang, K. 2012. Testing whether linear equations are causal: A free probability theory approach. *arXiv preprint arXiv:1202.3779*.